

Altered selectivity of a dipicolylamine based metal ion receptor

Joydev Hatai and Subhajit Bandyopadhyay*

Indian Institute of Science Education and Research (IISER) Kolkata, Mohanpur, Nadia, WB 741252, India,

E-mail: sb1@iiserkol.ac.in

Contents

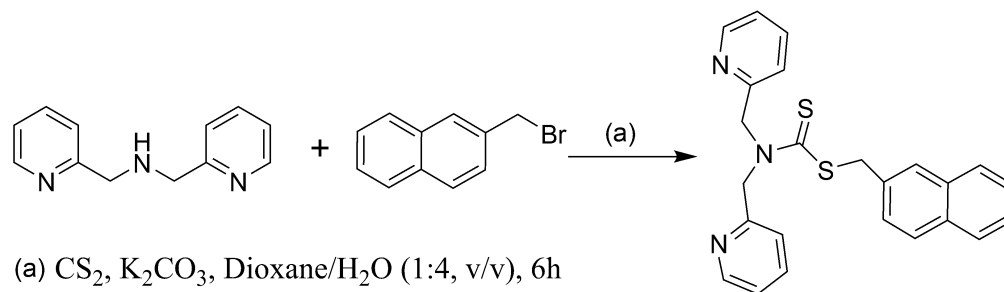
Instruments and Reagents.....	S3
Synthesis.....	S4
Figure S1.....	S6
Figure S2.....	S6
Figure S3.....	S7
Figure S4.....	S8
Figure S5.....	S9
Figure S6.....	S9
Figure S7.....	S10
Figure S8.....	S10
Figure S9A.....	S11
Figure S9B.....	S2711
Figure S10.....	S12
Figure S11.....	S12
Determination of dissociation constants.....	S13
Figure S12A.....	S13
Figure S12B.....	S14
Figure S12C.....	S14
Detection limit.....	S15
Figure S13.....	S15
Dynamic light scattering studies.....	S15

Figure S14A.....	S16
Atomic Force Microscopy (AFM).....	S16
Scanning electron microscope (SEM).....	S16
Fluorescence lifetime measurements.....	S17
Figure S14B.....	S2717
Table S1.....	S18
Crystallographic Details.....	S18
Table S2.....	S19
Table S3.....	S19
Table S4.....	S19
Figure S15.....	S20
Figure S16.....	S20
Figure S17.....	S21
Figure S18.....	S22
Figure S19.....	S23
Figure S20.....	S25
Figure S21.....	S27
Figure S22.....	S27
Figure S23.....	S27
Figure S24.....	S27
Figure S25.....	S27
Figure S26.....	S27
Figure S27.....	S27
Figure S28.....	S2730

Instruments and Reagents

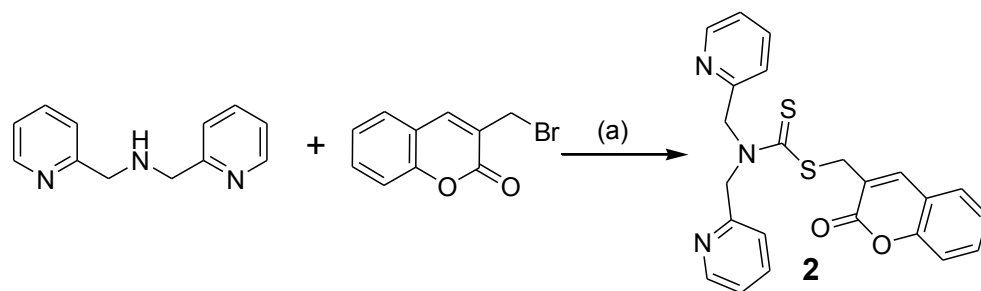
All reactants and reagents were commercially available and were used without further purification unless otherwise indicated. Solvents used were purified and dried by standard methods. The structures of the compounds were determined by 1D and 2D nuclear magnetic resonance spectroscopy and other spectroscopic techniques. ^1H and ^{13}C NMR spectra were recorded with 400 MHz Jeol and 500 MHz Bruker instrument. Chemical shifts are reported in δ values relative to an internal reference of tetramethylsilane (TMS) for ^1H NMR, and the solvent peak in ^{13}C NMR. The solvents for the spectroscopy experiments were of the spectroscopic grades and were free from any fluorescent impurities. Double distilled water was used for the spectroscopy experiments. The solutions of metal ions were prepared from $\text{Al}(\text{NO}_3)_3 \cdot 9\text{H}_2\text{O}$, $\text{LiClO}_4 \cdot 3\text{H}_2\text{O}$, NaClO_4 , $\text{Fe}(\text{ClO}_4)_3 \cdot x\text{H}_2\text{O}$, KClO_4 , $\text{Ba}(\text{NO}_3)_2 \cdot 4\text{H}_2\text{O}$, $\text{Mn}(\text{ClO}_4)_2$, $\text{Fe}(\text{ClO}_4)_2 \cdot x\text{H}_2\text{O}$, $\text{Co}(\text{ClO}_4)_2 \cdot 6\text{H}_2\text{O}$, $\text{Cd}(\text{NO}_3)_2$, AgNO_3 , $\text{Hg}(\text{NO}_3)_2$, $\text{Pb}(\text{ClO}_4)_2$, $\text{Ca}(\text{ClO}_4)_2 \cdot 4\text{H}_2\text{O}$, $\text{Cu}(\text{ClO}_4)_2 \cdot 6\text{H}_2\text{O}$, $\text{Ni}(\text{ClO}_4)$ and $\text{Zn}(\text{ClO}_4)_2 \cdot 6\text{H}_2\text{O}$ in H_2O . IR data were obtained with a FT-IR Perkin-Elmer spectrometer. UV spectra were recorded with a Cary 300Bio UV-vis spectrophotometer. Fluorescence measurements were carried out with Horiba Jobin Yvon (Fluoromax-3, Xe-150 W, 250-900 nm). Mass spectrometry data were obtained from an AcquityTM ultra performance LCMS. pH data were recorded with a Sartorius Basic Meter PB-11 calibrated at pH 4, 7 and 10. Reactions were monitored by thin layer chromatography using Merck plates (TLC Silica Gel 60 F₂₅₄). Developed TLC plates were visualized with UV light (254 nm). Silica gel (100 ~ 200 mesh, Merck) was used for column chromatography. Yields refer to the chromatographically and spectroscopically pure compounds, unless indicated.

Reaction Scheme



Synthesis

Compound **1** was synthesized following the reported method of thiocarbamate synthesis.¹ Dipicolylamine (0.1 g, 0.09 mL, 0.50 mmol) and K_2CO_3 (0.35 g, 2.50 mmol) in dioxane/water (1:4, v/v) was stirred for 5 minutes at 0°C. Carbon disulfide (0.76 g, 0.60 mL, 10.0 mmol) was added and the mixture was stirred for another 5 minutes. 2-(bromomethyl)naphthalene (0.12 g, 0.50 mmol) dissolved in dioxane was subsequently added to it dropwise over a period of 10 minutes. The solution was allowed to attain room temperature (25°C) and stirred for another 30 minutes. After the disappearance of the spot for the starting materials in TLC, the solution was concentrated under reduced pressure. The yellowish solid thus obtained was dissolved in dichloromethane (20 mL) and washed with water. The organic layer was dried over anhydrous Na_2SO_4 and the volatiles were removed under reduced pressure, which on chromatography ($\text{CH}_2\text{Cl}_2/\text{CH}_3\text{CN}$, 8:2, v/v) yielded compound **1** as a white solid (0.19 g, 82%) which was subsequently crystallized and the structure was solved (CCCD # 942550); mp 118-120°C. ^1H NMR (400 MHz, CDCl_3) δ 8.55 (s, 2H, ArH), 7.78(m, 4H, ArH), 7.62 (m, 2H, ArH), 7.46 (m, 4H, ArH), 7.18 (m, 3H, ArH), 5.5 (s, 2H, ArCH₂), 5.23 (s, 2H, ArCH₂), 4.75 (s, 2H, ArCH₂). ^{13}C NMR (125 MHz, CDCl_3) δ : 199.2, 155.5, 154.7, 149.7, 149.4, 133.0, 132.6, 128.2, 128.1, 127.7, 127.6, 127.2, 126.2, 125.9, 122.5, 59.2, 57.1, 43.2. λ_{abs} in MeOH (nm, ϵ): 260 (20000), 370 (1200). FT-IR (KBr, cm^{-1}): 2923, 2852, 1593, 1474, 1436, 1400, 770, 753. ESI-MS calculated for $\text{C}_{24}\text{H}_{21}\text{N}_3\text{S}_2\text{Na}^+$ 438.1, found 438.2.



(a) CS₂, K₂CO₃, Dioxane/H₂O (1:4, v/v), 6h

The similar procedure was follow for the preparation of compound **2**. Dipicolylamine (0.1 g, 0.09 mL, 0.50 mmol) and K₂CO₃ (0.35 g, 2.50 mmol) in dioxane/water (1:4, v/v) was stirred for 5 minutes at 0°C. Carbon disulfide (0.76 g, 0.60 mL, 10.0 mmol) was added and the mixture was stirred for another 5 minutes. 3-(bromomethyl)coumarin (0.119 g, 0.50 mmol) dissolved in dioxane was subsequently added to it dropwise over a period of 10 minutes. The solution was allowed to attain room temperature (25°C) and stirred for another 30 minutes. The yellowish reaction mixture was concentrated under reduced pressure. The yellowish solid thus obtained was dissolved in dichloromethane (20 mL) and washed with water. The organic layer was dried over anhydrous Na₂SO₄ and the volatiles were removed under reduced pressure, which on chromatography (CH₂Cl₂/C₆H₁₂, 8:2, v/v) yielded compound **2** as a white solid (0.20 g, 92%); mp 134-136°C. ¹H NMR (400 MHz, CDCl₃) δ: 8.54 (m, 2H, ArH), 8.00 (s, 1H, ArH), 7.64 (m, 2H, ArH), 7.46 (m, 2H, ArH), 7.37 (m, 1H, ArH), 7.27 (m, 3H, ArH), 7.17 (m, 2H, ArH), 5.53 (s, 2H, ArCH₂), 5.23 (s, 2H, ArCH₂), 4.57 (s, 2H, ArCH₂). ¹³C NMR (125 MHz, CDCl₃) δ: 198.8, 161.3, 155.4, 154.6, 153.4, 149.8, 149.5, 141.2, 136.9, 131.4, 128.0, 124.5, 122.7, 122.6, 121.6, 119.2, 116.5, 59.7, 57.2, 37.0. FT-IR (KBr, cm⁻¹): 3041, 3005, 2981, 2928, 1720, 1608, 1589, 1482, 1431, 1402, 1215, 1178, 1063, 755. ESI-MS calculated for C₂₃H₁₉N₃S₂H⁺ 434.1, found 434.1.

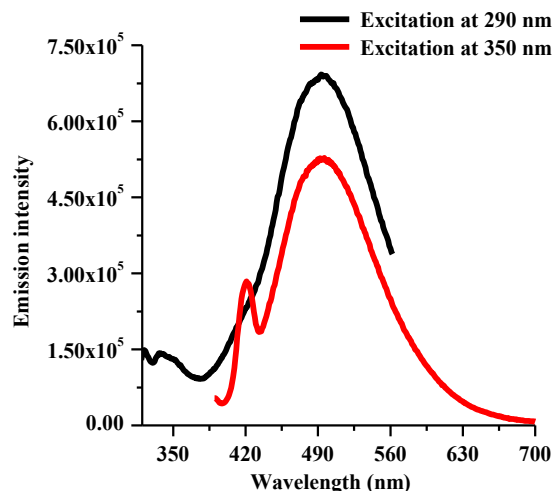


Figure S1. Fluorescence spectra of chemosensor **1** ($10 \mu\text{M}$) on excitation with at 290 nm and 350 nm in mixed aqueous-organic solvent media ($\text{H}_2\text{O}/\text{MeOH}$, 3:2, v/v) with 1% DMSO as a co-solvent buffered at pH 7.0 with HEPES (1 mM) at 25°C . The excitation of **1** at these two wavelengths does not change the emission maximum.

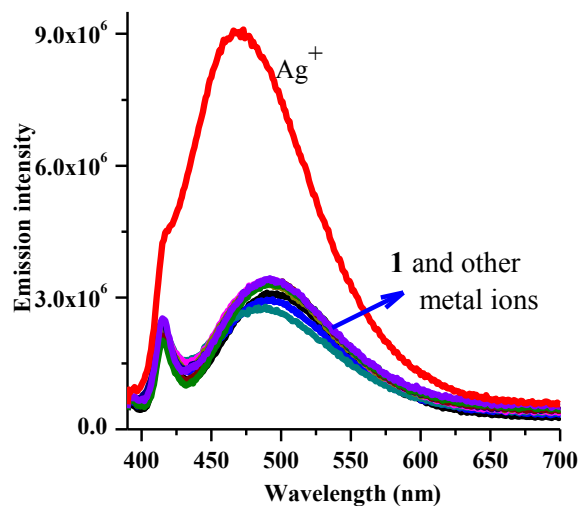


Figure S2. Change in fluorescence intensity of **1** ($10 \mu\text{M}$) upon addition of various metal ions ($10 \mu\text{M}$) in MeOH with 1% DMSO as a co-solvent at 25°C .

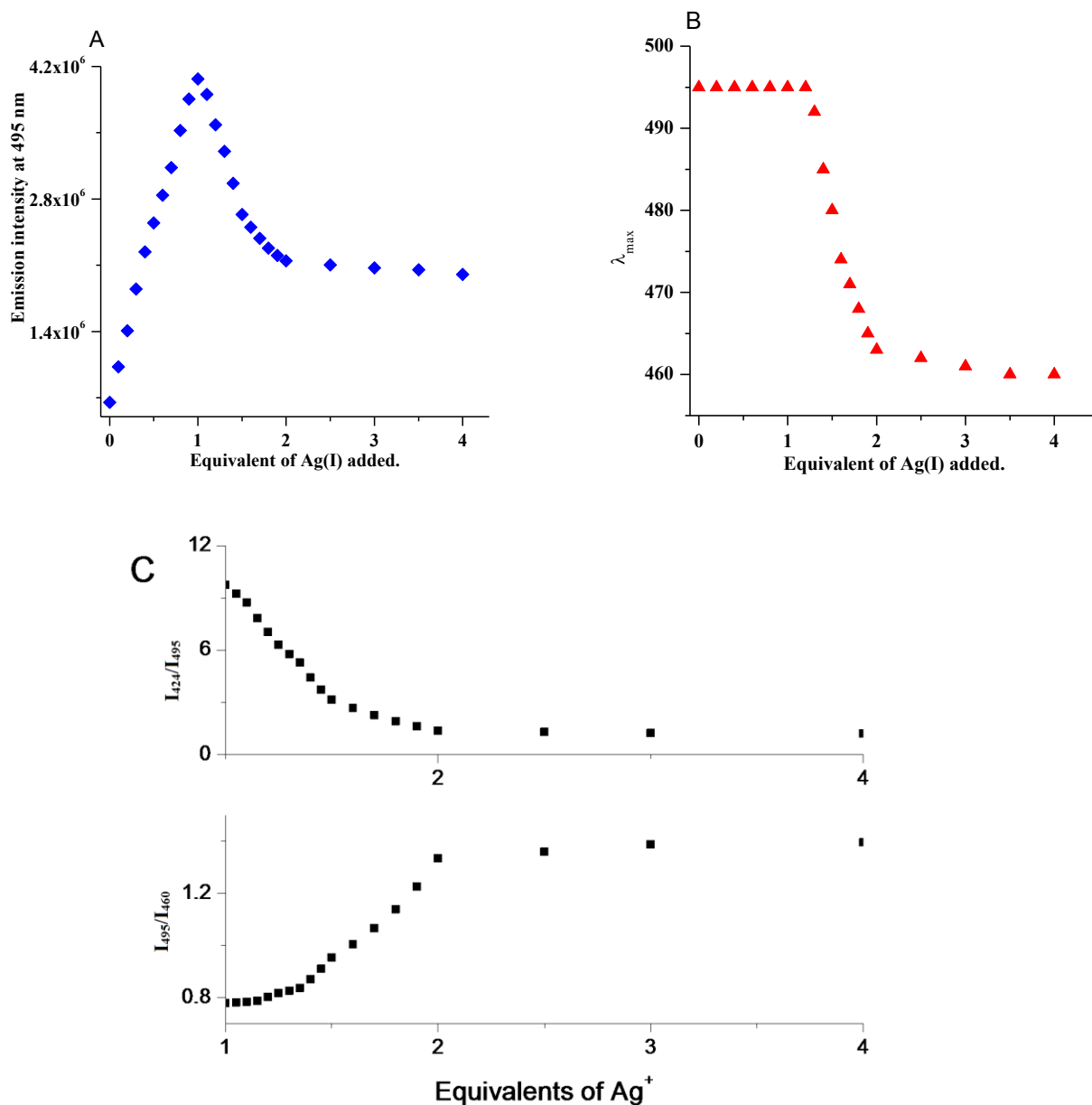


Figure S3. Change in the emission intensity (A) and fluorescence maximum (B) of **1** (10 μM) upon addition of increasing amounts of Ag⁺ (0 to 5.0 equivalent) in mixed aqueous-organic solvent media (H₂O/MeOH, 3:2, v/v) with 1% DMSO as a cosolvent buffered at pH 7.0 with HEPES (1mM) at 25 °C. (C) Double ratiometric behavior of the sensor in mixed solvent media.

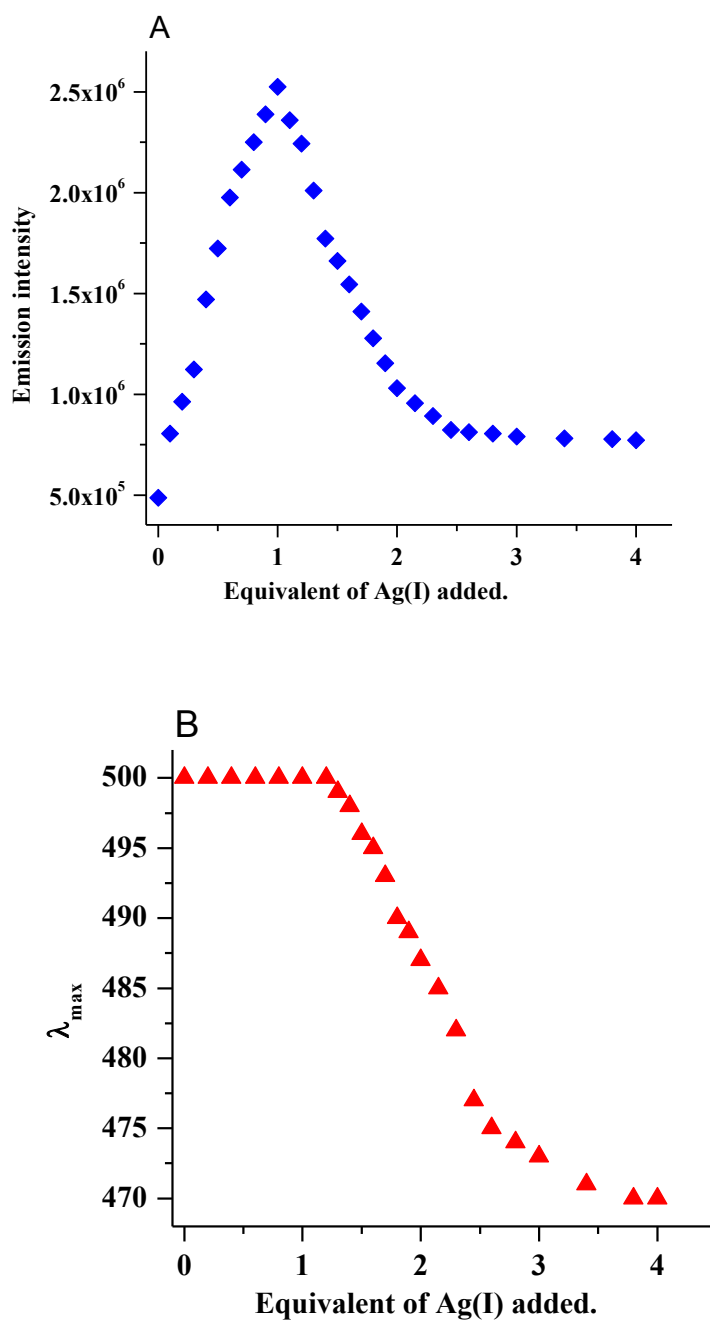


Figure S4. Change in the emission intensity (A) and fluorescence maximum (B) of **1** ($10 \mu\text{M}$) upon addition of different equivalent of Ag^+ (0 to 5.0 equivalent) in water with 1% DMSO as a cosolvent buffered at pH 7.0 with HEPES (1mM) at $25 \text{ }^\circ\text{C}$.

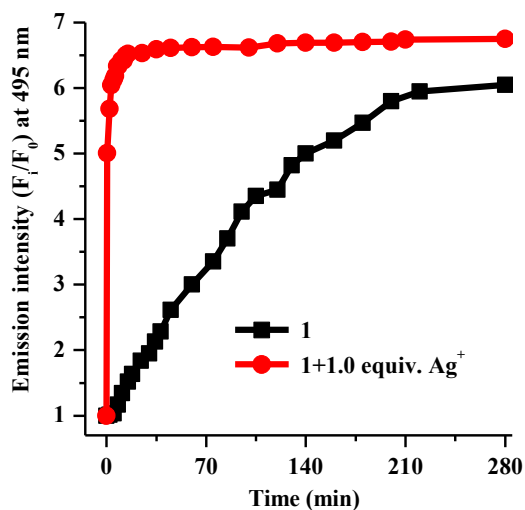


Figure S5. Time dependent fluorescence change of chemosensor **1** (10 μM) and **1**.Ag⁺ (1 equivalent) in mixed aqueous-organic solvent media (H₂O/MeOH, 3:2, v/v) with 1% DMSO as a cosolvent buffered at pH 7.0 with HEPES (1mM) at 25°C.

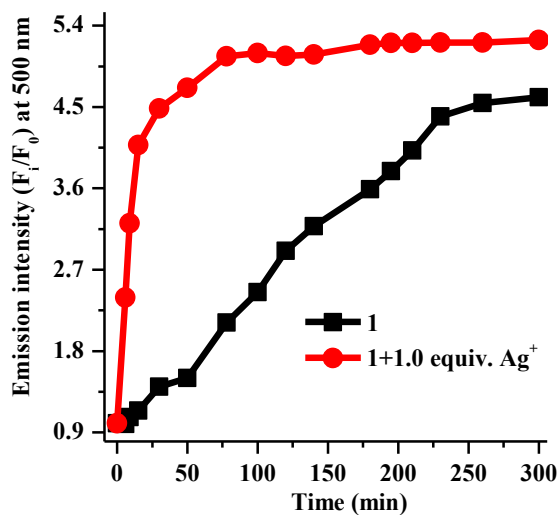


Figure S6. Time dependent fluorescence change of chemosensor **1** (10 μM) and **1**.Ag⁺ (1 equivalent) in aqueous media with 1% DMSO as a cosolvent buffered at pH 7.0 with HEPES (1mM) at 25 °C.

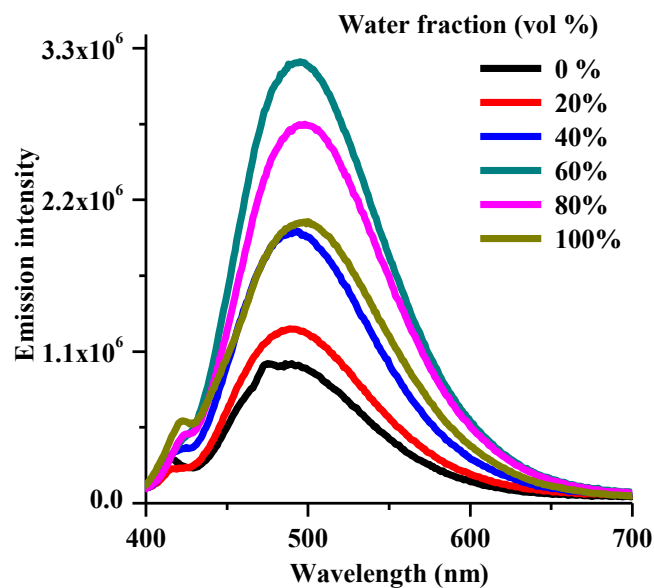


Figure S7. Fluorescence emission spectra of **1** (10 μM) in different ratios of H₂O/MeOH at $\lambda_{\text{ex}} = 350$ nm.

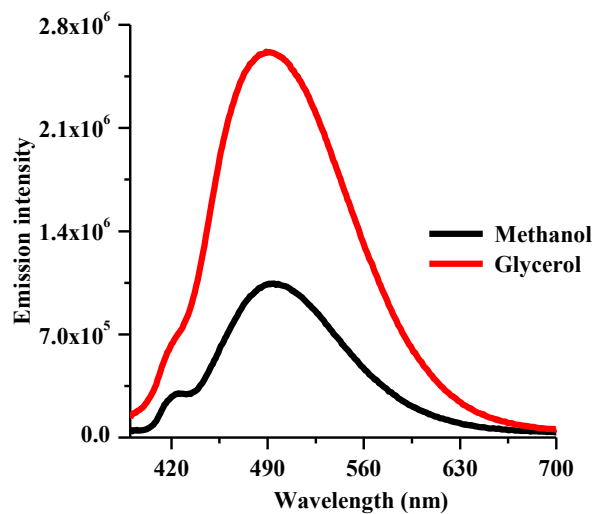


Figure S8. Fluorescence spectra of chemosensor **1** (10 μM) in glycerol and methanol $\lambda_{\text{ex}} = 350$ nm.

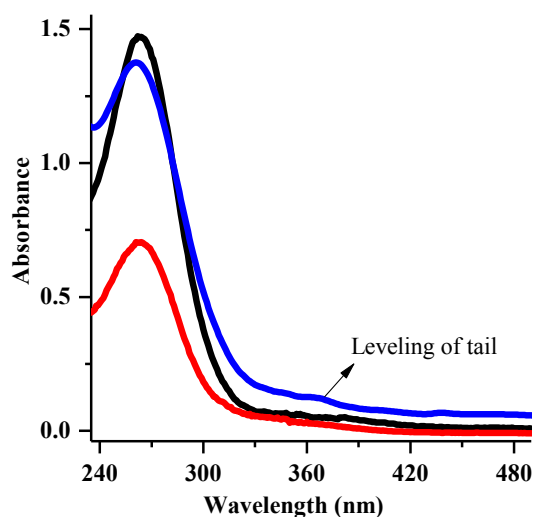


Figure S9A. The changes in the UV-vis absorption spectrum of chemosensor **1** (10 μM) (at 0 min, *red line*) upon titration with Ag^+ (1 equiv. *blue line* and 5 equiv. *black line*) in mixed solvent media ($\text{H}_2\text{O}/\text{MeOH}$, 3:2, v/v) with 1% DMSO as a cosolvent buffered at pH 7.0 with HEPES (1 mM) at 25 $^\circ\text{C}$.

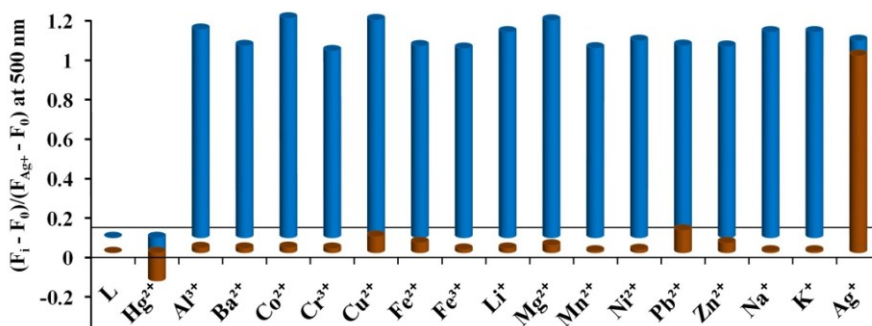


Figure S9B. Fluorescence response of **1** (10 μM) upon addition of various metal ions (10 μM) (*Brown bar*) and restoration of fluorescence of **1** (10 μM) towards Ag^+ (10 μM) in presence of various metal ions (50 μM) (*blue bar*) in mixed solvent media.

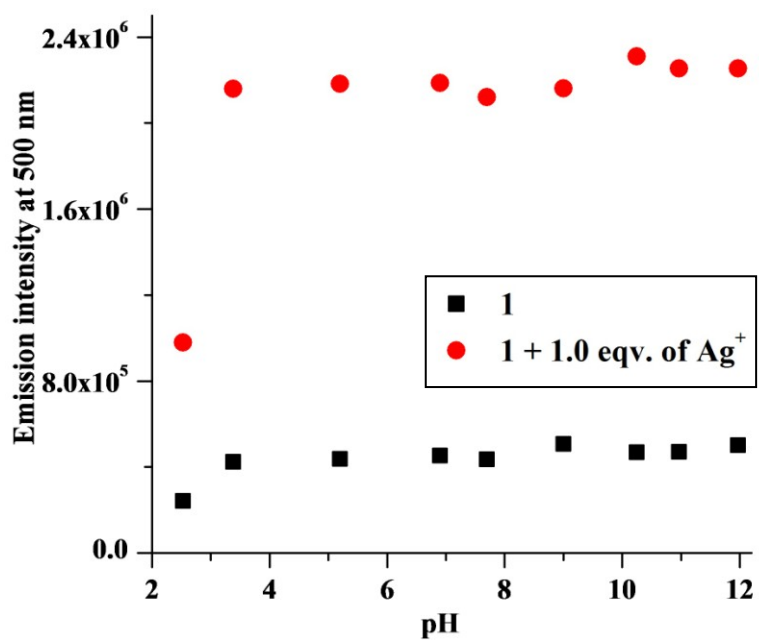


Figure 10. Change in the fluorescence intensity of **1** (10 μ M) and **1**.Ag⁺ with pH .

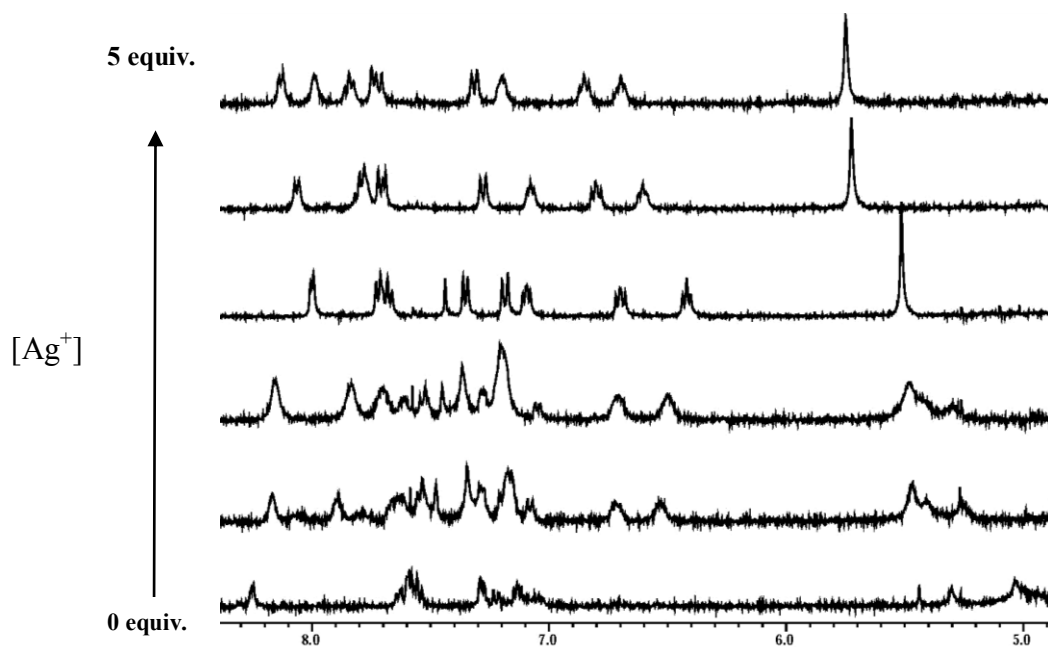


Figure S11. ¹H NMR titration of sensor **1** (1 mM) with Ag⁺ ion (0, 0.3, 0.6, 1.0, 2.0, 5.0 equiv. respectively) in MeOD/D₂O (1:1, v/v) at 25°C

Determination of dissociation constants

The association (K_a) and the dissociation constant ($K_d = 1/K_a$) of Ag^+ was determined from the fluorescence titration experiment using the following equation², $(F_i - F_0) = \Delta F = [Ag^+](F_{max} - F_0)/(K_d + [Ag^+])$. F_i is the observed fluorescence with varying amounts of Ag^+ , F_0 is the fluorescence for the free chemosensor **1**, F_{max} is the saturation value of the fluorescence intensity for the metal complexes. To obtain $y = Ax + B$ a linear equation, the reciprocal of ΔF was plotted against the reciprocal of the concentration of Ag^+ . K_d was calculated from the ratio A/B .

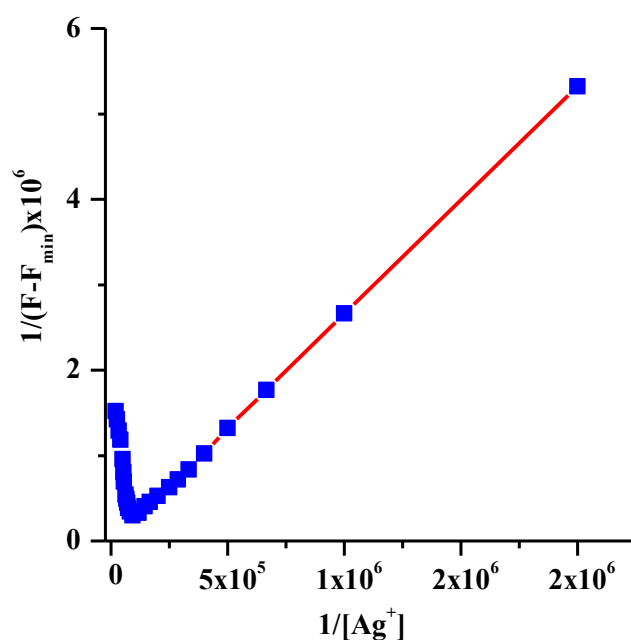


Figure S12A. Reciprocal plot from the titration data of **1** ($10 \mu\text{M}$) with Ag^+ (0 to 5.0 equivalents) in mixed solvent medium ($H_2O/MeOH$, 3:2, v/v) buffered at pH 7.0 with HEPES (1 mM) at 25°C clearly shows a break at 1.0 equivalent of Ag^+ . The two slopes with opposite trends also indicate an association and a dissociation process in the respective concentration range of Ag^+ .

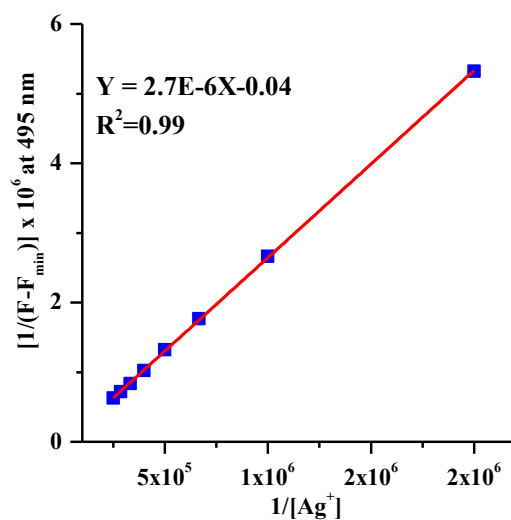


Figure S12B. Plot for calculation of association constant of **1** (10 μ M) with Ag^+ (0 to 1.0 equivalent) in mixed solvent medium ($H_2O/MeOH$, 3:2, v/v) buffered at pH 7.0 with HEPES (1 mM) at 25 $^\circ$ C.

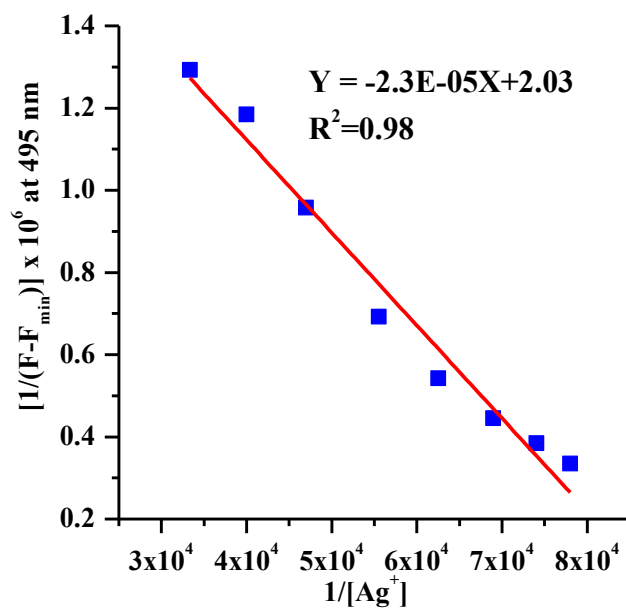


Figure S12C. Plot for calculation of dissociation constant of **1** (10 μ M) with Ag^+ (1.0 to 5.0 equivalent) in mixed solvent medium ($H_2O/MeOH$, 3:2, v/v) with 1% DMSO as a cosolvent buffered at pH 7.0 with HEPES (1 mM) at 25 $^\circ$ C.

Detection limit

The detection limit for the ions was calculated from the titration experiments following the reported method.³ For Ag^+ in mixed aqueous-organic ($\text{H}_2\text{O}/\text{MeOH}$, 3:2, v/v), the fluorescence intensity data at 495 nm were normalised between the minimum intensity found at zero equivalent of Ag^+ and the maximum intensity found at 1 equivalent of Ag^+ added. A linear curve was obtained from these normalized fluorescence intensity data and the intercept on the X-axis was considered as the detection limit. Thus the value obtained for the Ag^+ was found to be 8.3×10^{-8} (M).

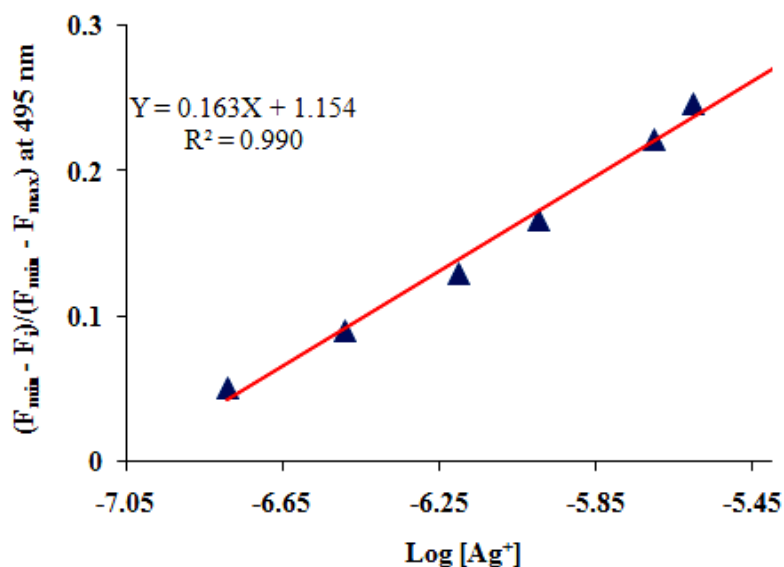


Figure S13. Determination of detection limit of chemosensor **1** (10 μM) from fluorescence titration in mixed solvent medium ($\text{H}_2\text{O}/\text{MeOH}$, 3:2, v/v) with 1% DMSO as a cosolvent buffered at pH 7.0 with HEPES (1 mM) at 25 °C. The detection limit of chemosensor is 83 nM.

Dynamic light scattering studies

The particle size of the aggregates was measured by dynamic light scattering (DLS) experiments on a Malvern Zetasizer Nano ZS instrument equipped with a 4.0 mW He–Ne laser operating at a wavelength of 633 nm. The samples and the background were measured at room temperature (25 °C) at a scattering angle of 173°. DLS experiments were carried out with an optically clear solution of **1** (10 μM) in MeOH, mixed aqueous-organic and H_2O medium in the presence and absence of the Ag^+ ion. The solution was equilibrated for 30 minutes before taking the measurements.

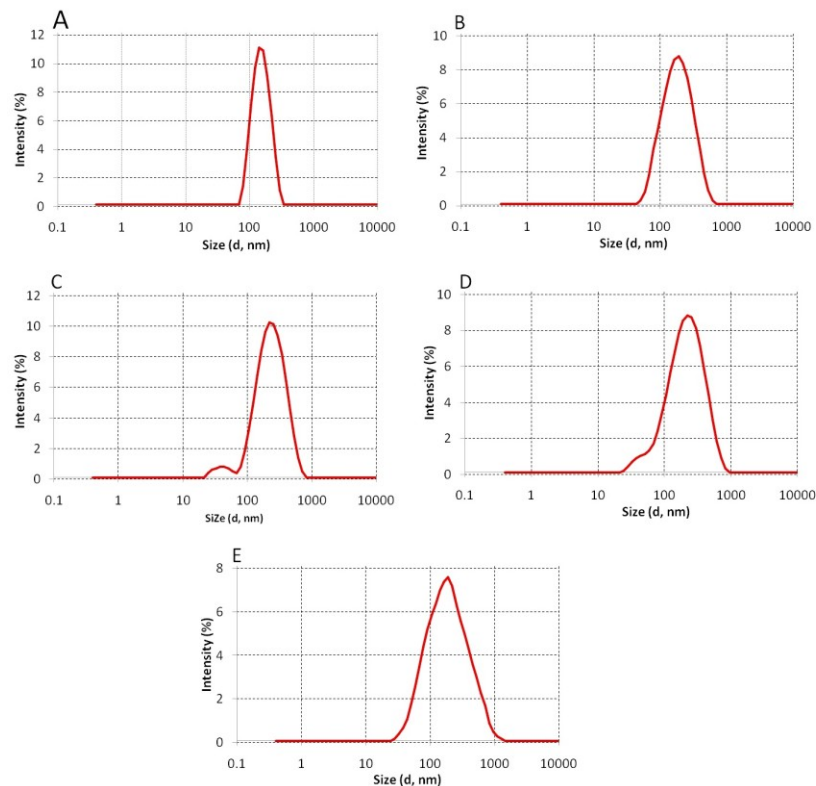


Figure S14A. DLS measurements of **1** (10 μ M) in various ratio of MeOH/H₂O at 25 °C [(A) 60:40, (B) 50:50, (C) 40:60, (D) 30:70, (E) 20:80] The sizes obtained from the DLS studies were 157 (0.325), 181 (0.447), 239 (0.310), 222 (0.324), 212 (PDI 0.529).

Atomic Force Microscopy (AFM) Studies

The overall morphology of the **1** was investigated from NT-MDT micro-40 AFM instrument using a semicontact mode at a scan rate of 1 Hz. A solution of **1** (10 μ M) in mixed aqueous-organic (H₂O/MeOH, 3:2, v/v) medium was drop-casted on cover slip and left open to atmosphere for 12 h, followed by desiccators before taking AFM images.

Scanning Electron Microscope (SEM) Studies

The morphology of the **1** was determination from a Jeol JEM 6700 field emission scanning electron microscope (FE-SEM) with attached an energy dispersive X-ray spectroscopic (EDS). A solution of **1** (10 μ M) in mixed aqueous-organic (H₂O/MeOH, 3:2, v/v) solvent was drop-casted on cover slip and left open to atmosphere for 12 h, followed by desiccators prior to taking SEM images.

Fluorescence lifetime measurements

The fluorescence lifetime was recorded using a time correlated single-photon counting (TCSPC) spectrometer (Horiba Jobin Yvon IBH). Fluorescence lifetime of **1** (10 μM) in methanol and mixed aqueous-organic ($\text{H}_2\text{O}/\text{MeOH}$, 3:2, v/v) solvent was carried out in the presence and absence of the Ag^+ (10 μM and 50 μM) ion. A laser ($\lambda_{\text{ex}} = 375 \text{ nm}$) was used as the excitation source and a MCP photomultiplier tube (PMT) (Hamamatsu R3809U-50 series) was employed as the detector. IRF was recorded using a scatterer (dilute solution of Ludox in water). Nonlinear least-squares iterative reconvolution procedure using IBH DAS6 (Version 2.2) was used in order to fit the fluorescence decay curves using a general triexponential decay equation. The quality of the fit was assessed from the χ^2 values.

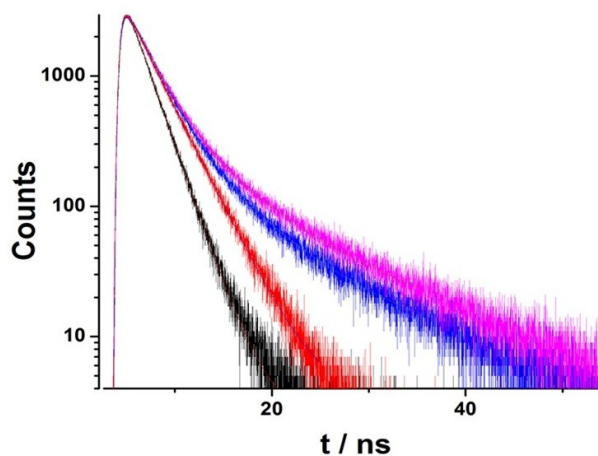


Figure S14B. Fluorescence lifetime experiments **1** (10 μM), see text.

In methanol, a degassed solution of **1** (10 μM) showed a mono-exponential decay profile of the excited states with a lifetime of 1.62 ns (τ_1) (Figure S14B, black decay trace). This corresponds to the lifetime of the non-aggregated monomers. In $\text{H}_2\text{O}/\text{MeOH}$ (3:2, v/v), the decay profile showed a bi-exponential nature with two lifetimes of 1.79 (τ_1) and 7.71 ns (τ_2) (Figure S14B, purple decay trace). The relaxation through the slower channel increased as the data were collected at longer time intervals (0, 1.5h and 3h) indicating that the τ_2 values corresponded to the lifetime of the aggregated species (Table S1). In presence of one equivalent of Ag^+ , the τ_2 value was somewhat less (6.02 ns) (Figure S14B, blue decay trace), however the decay was

largely through this channel. On addition of 5 equivalents of Ag^+ , the relaxation was predominantly through the faster channel 2.01 ns (τ_1) indicating that the disintegration of the aggregates and formation of monomeric species (Figure S14B, red decay trace).

Table S1. Fluorescence lifetime of **1** and **1**. Ag^+ under various conditions

Solvent (% vol.)	Time (h)	Ag^+ (equiv.)	$\tau_1(\text{ns})/A_1^{[a]}$	$\tau_2(\text{ns})/A_2$	χ^2
MeOH : H ₂ O (100:0)	-	-	1.62 (100)	-	1.13
MeOH : H ₂ O (40:60)	1.5	0	1.79 (72)	7.71(28)	1.05
MeOH : H ₂ O (40:60)	3	0	1.86 (37)	7.76(63)	1.07
MeOH : H ₂ O (40:60)	-	1.0	1.83 (35)	6.02 (65)	1.03
MeOH : H ₂ O (40:60)	-	5.0	2.01 (100)	-	1.08

[a] τ and A values represents the fluorescence lifetimes and percentage fraction amounts of the short (1) and the long (2) lived species.

Crystallographic Details: (CCDC Number 942550)

Crystal Data were collected on a Bruker SMART APEXII CCD area-detector diffractometer using graphite monochromated Mo K_α radiation ($\lambda = 0.71073 \text{ \AA}$). For both the crystals, X-ray data reduction was carried out using the Bruker SAINT program. The structures were solved by direct methods using the SHELXS-97 program and refinement using SHELXL-97 program. Selected crystal and data collection parameters for all the complexes are given in **Table S2**. X-ray data reduction, structure solution and refinement were done using the SHELXL-97 program package. Selected bond lengths and bond angles of compound **1** are given in **Table S3** and **Table S4** respectively.

Compound **1**: Single crystals were obtained by slow diffusion of CH_3CN solution. The unit cell dimensions were determined by a least squares fit of 1141 machine centered reflections ($0^\circ < \theta < 20^\circ$) for sensor **1**. Thirty six standard reflections were used to check the crystal stability toward X-ray exposure showed no significant intensity reduction over the course of data collection. Five final cycles of refinement converged with discrepancy indices $R[F^2 > 2\sigma(F^2)] = 0.0446$ and $wR(F^2) = 0.0779$ for **1**.

Table S2: Crystallographic parameters for **1**

	1
Empirical formula	C ₂₄ H ₂₁ N ₃ S ₂
F.W.	415.58
space group	Monoclinic, P2(1)
<i>a</i> (Å)	6.2365(19)
<i>b</i> (Å)	8.196(3)
<i>c</i> (Å)	20.593(7)
β(°)	92.844(9)
<i>V</i> , Å ³	1051.3(6)
<i>Z</i>	2
λ, Å	0.71073
crystal size, mm ³	0.56×0.15×0.04
<i>T</i> , K	296(2)
μ, mm ⁻¹	0.269
R[F ² >2σ(F ²)]	0.0446
wR(F ²)	0.0779
GOF	1.002
w	1/[σ ² (F _o ²)+(0.0261P) ² +0.2164P] where P=(F _o ² +2F _c ²)/3

Table S3: Selected bond lengths (Å) of **1**

1			
S1	C13	1.772(3)	S2 C13 1.666(3)
S1	C14	1.809(4)	N3 C13 1.339(4)

Table S4: Selected bond angles (deg) of **1**

1							
C13	N3	C6	121.3(3)	N3	C13	S2	124.0(3)
C13	N3	C12	122.8(3)	N3	C13	S1	114.1(2)

C6	N3	C12	115.9(3)	S2	C13	S1	121.9(2)
C13	S1	C14	102.81(17)				

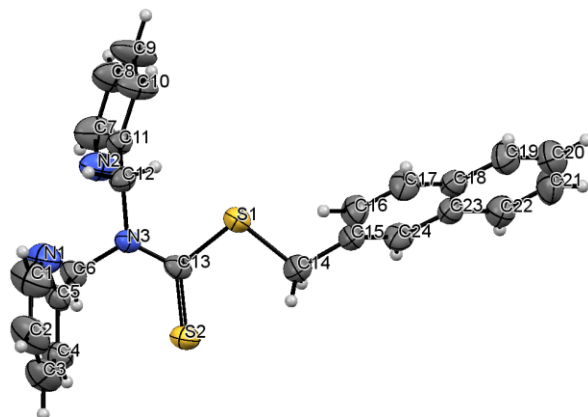


Figure S15: Crystal structure of **1** (thermal ellipsoid plot with 50% probability)

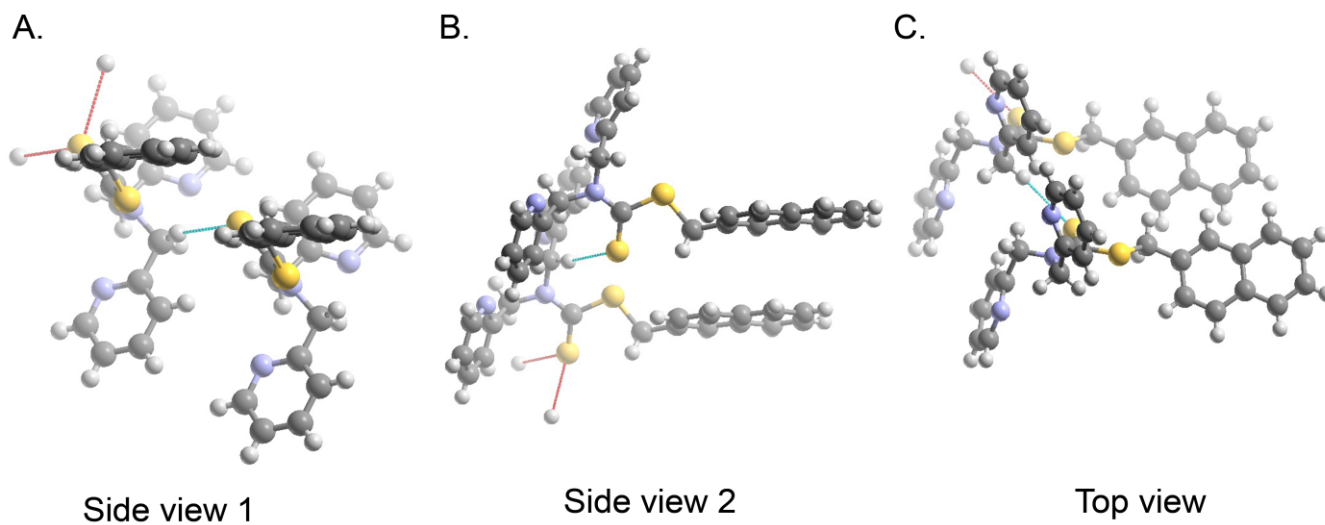


Figure S16: Two consecutive neighboring naphthalene units in the crystal of **1** are aligned in a parallel-displaced/parallel off set arrangement at a distance of 4.3 Å.

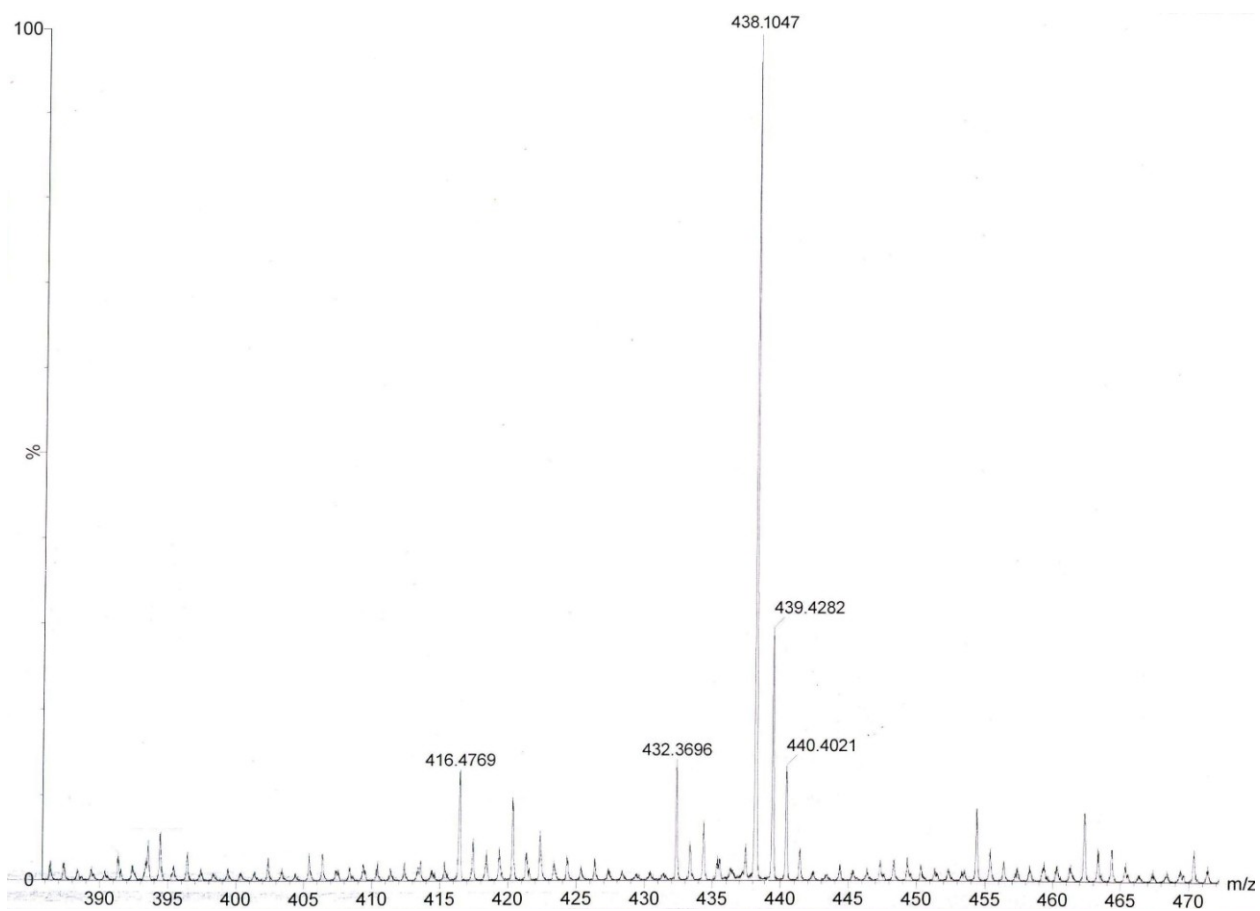


Figure S17. Mass spectrum of **1**

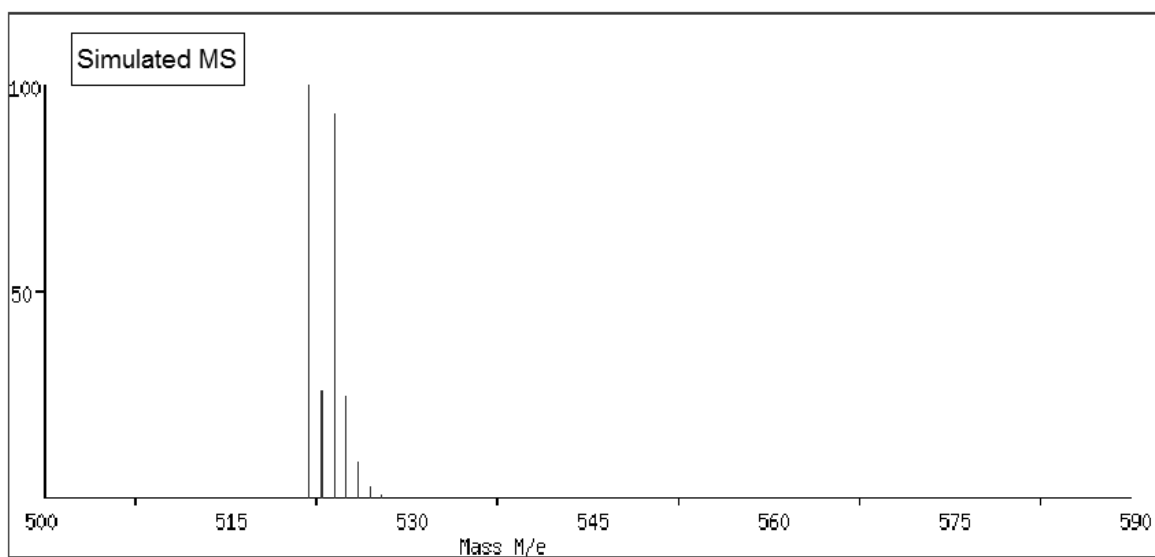
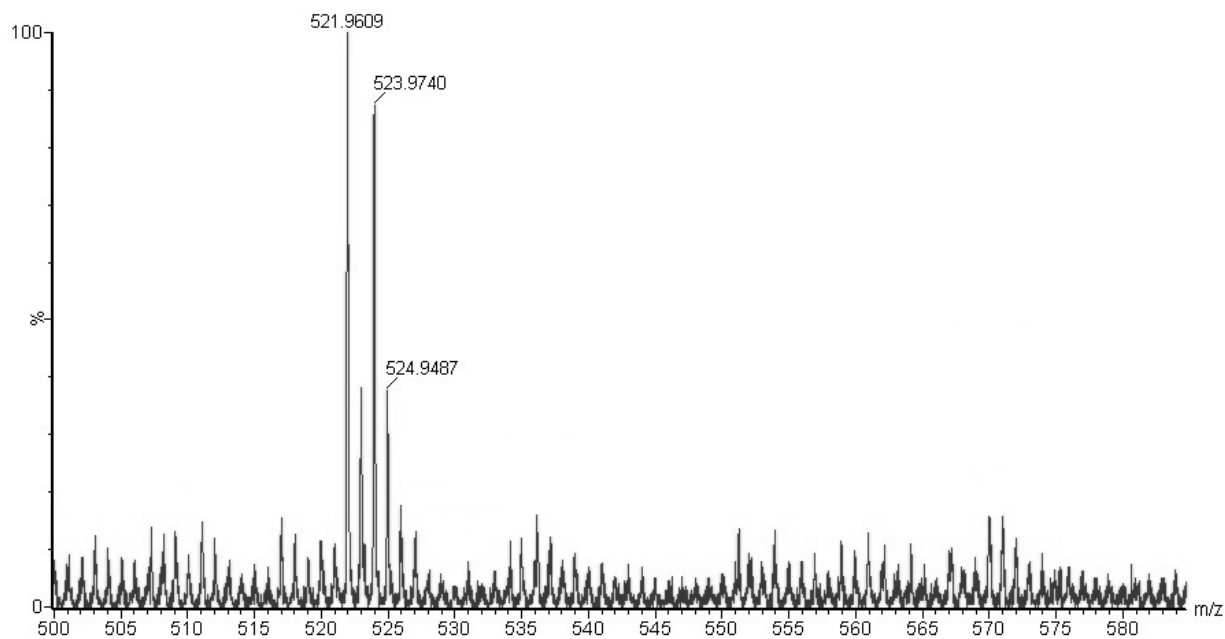


Figure S18. Mass spectrum of $1.Ag^+$ complex corresponding to $[1 + Ag]^+$. The spectrum below is the simulated spectrum that shows the matching isotope pattern.

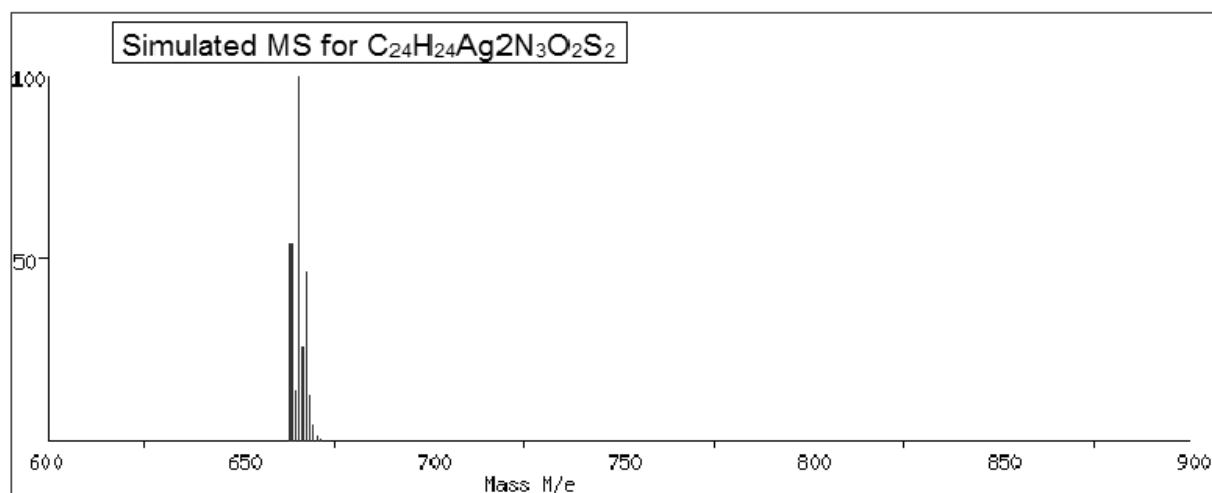
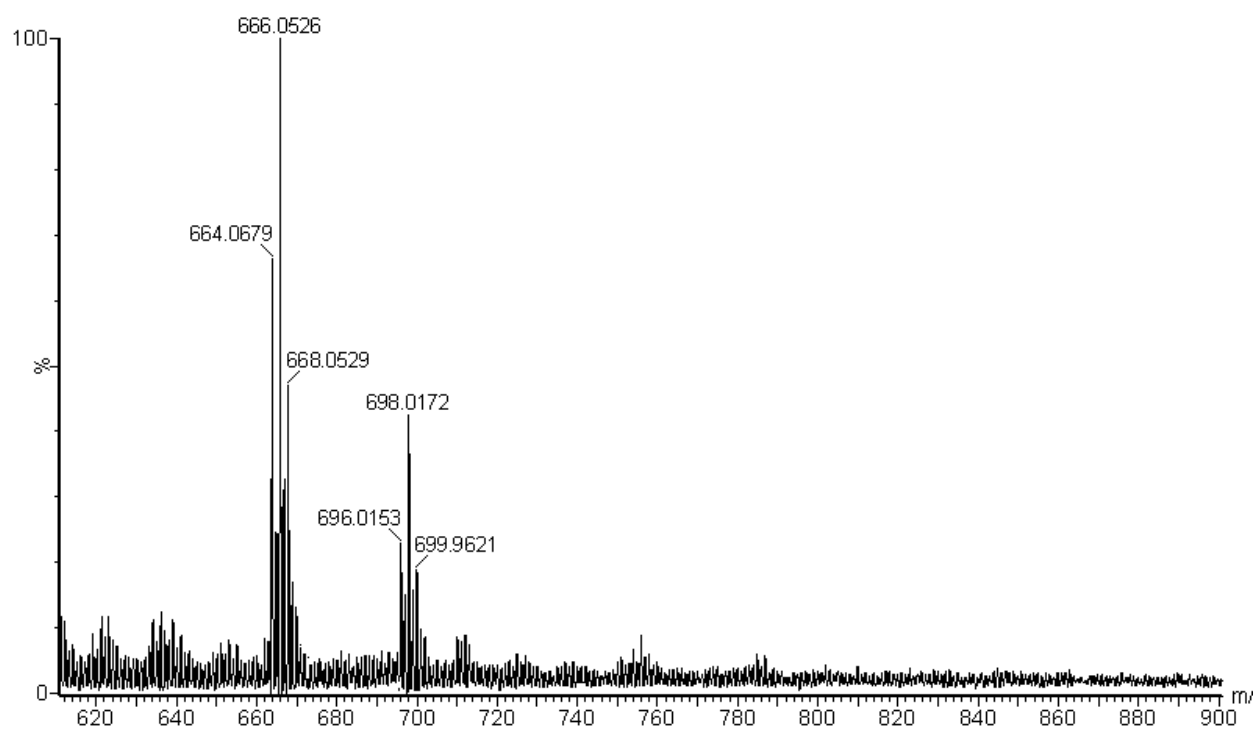


Figure S19. Mass spectrum of the complex corresponding to $[1 + 2Ag^+ + H_2O + OH^-]$. A peak at 32 amu higher corresponds to a methanol molecule associating with the cluster. The spectrum within the box is the simulated spectrum.

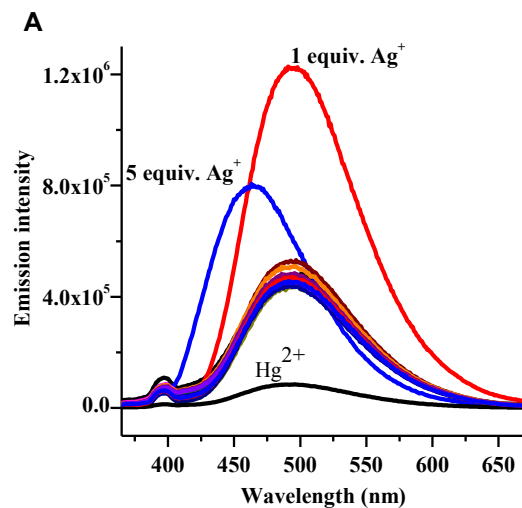


Figure 20. Change in fluorescence intensity of **2** (10 μM) upon addition of various metal ions (10 μM). The spectrum with Ag^+ in blue refers to the change on addition of 50 μM of Ag^+ in $\text{H}_2\text{O}/\text{MeOH}$, 3:2, v/v.

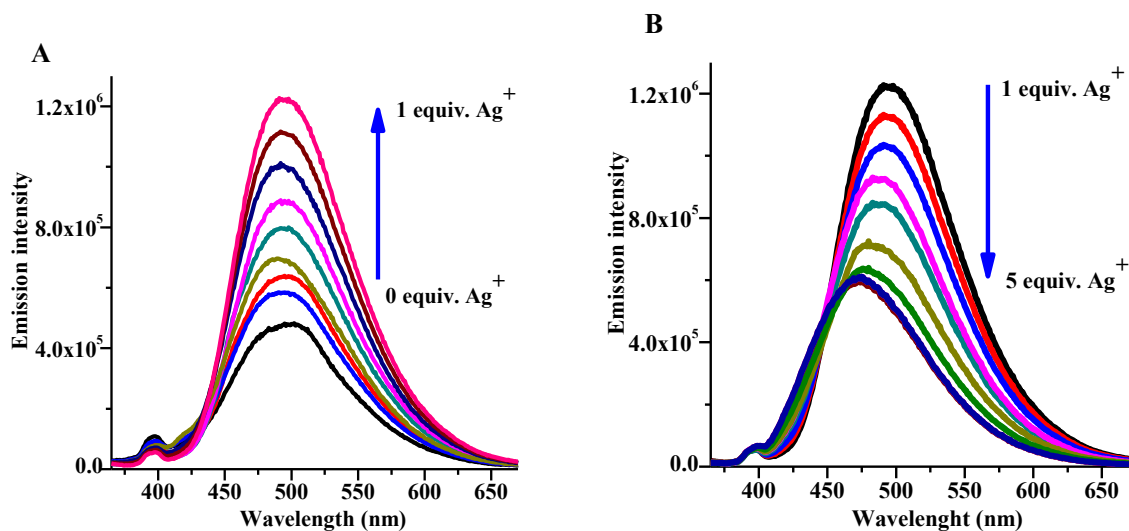


Figure 21. Change in fluorescence emission of **2** (10 μM) in $\text{H}_2\text{O}/\text{MeOH}$ (3:2, v/v) and on addition of (A) 0-1 equivalents and (B) 1-5 equivalents of Ag^+ .

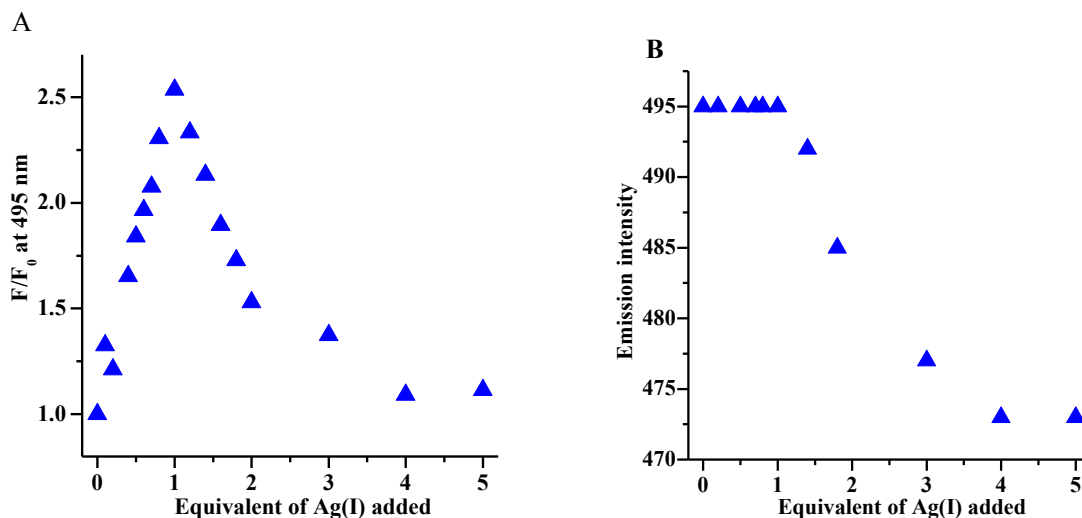


Figure 22. Change in the emission intensity (A) and fluorescence maximum (B) **2** (10 μ M) upon addition of increasing amounts of Ag^+ (0 to 5.0 equivalent) in mixed aqueous-organic solvent media ($\text{H}_2\text{O}/\text{MeOH}$, 3:2, v/v) with 1% DMSO as a cosolvent buffered at pH 7.0 with HEPES (1mM) at 25 $^\circ\text{C}$.

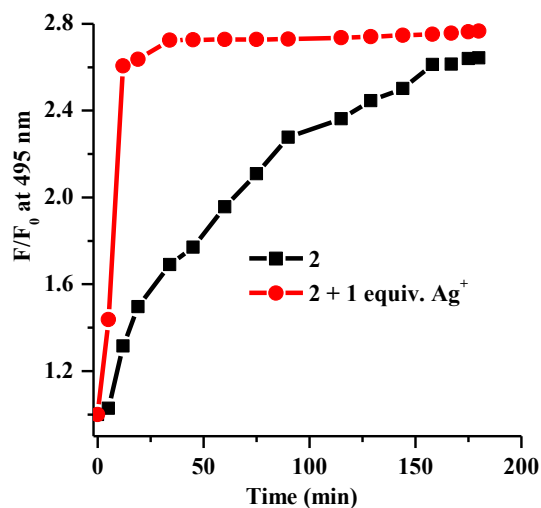


Figure 23. Time dependent fluorescence change of chemosensor **2** (10 μ M) and **2**. Ag^+ (1 equivalent) in mixed aqueous-organic solvent media ($\text{H}_2\text{O}/\text{MeOH}$, 3:2, v/v) with 1% DMSO as a cosolvent buffered at pH 7.0 with HEPES (1mM) at 25 $^\circ\text{C}$.

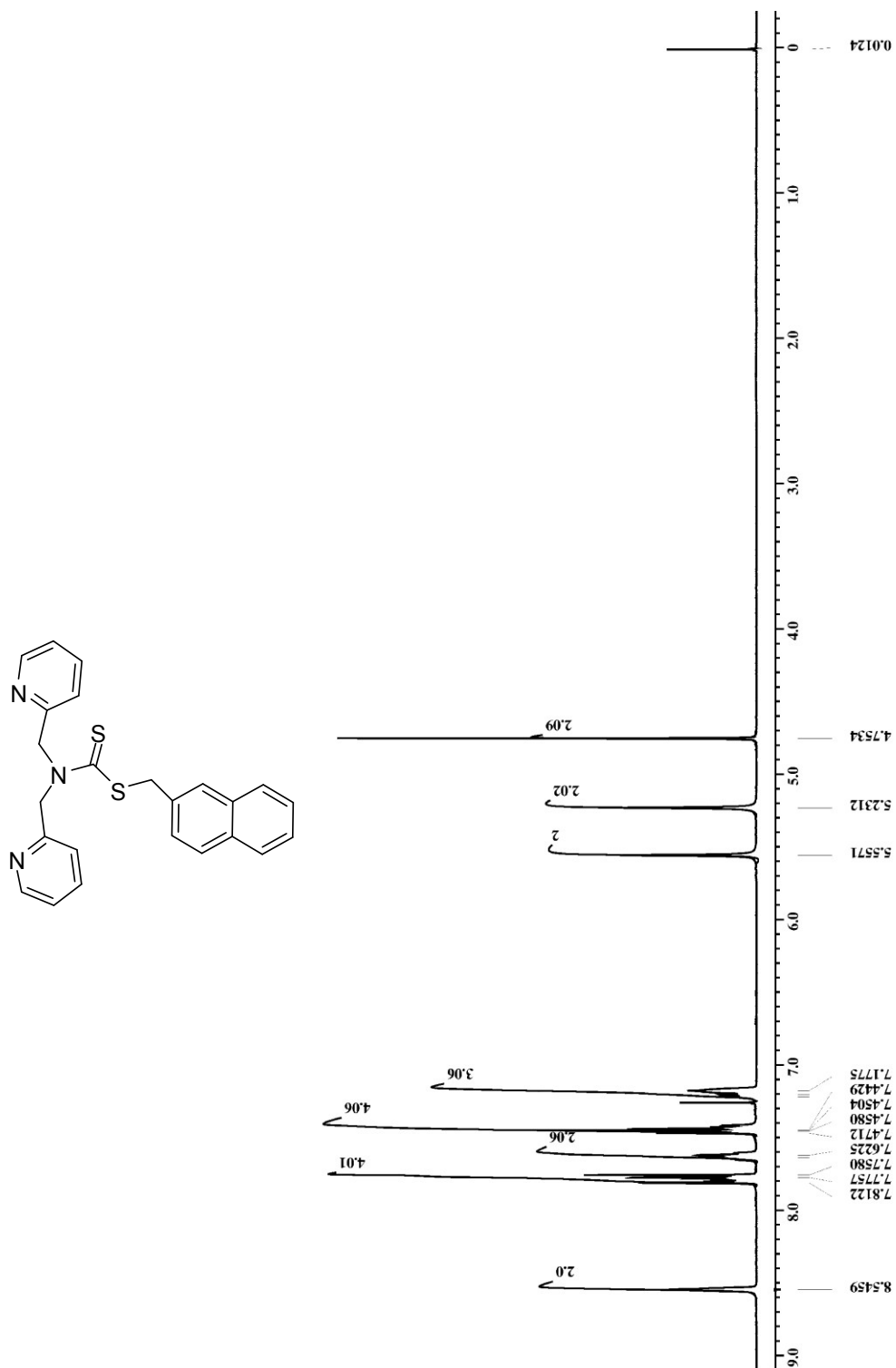


Figure S24. ¹H NMR spectrum of **1**

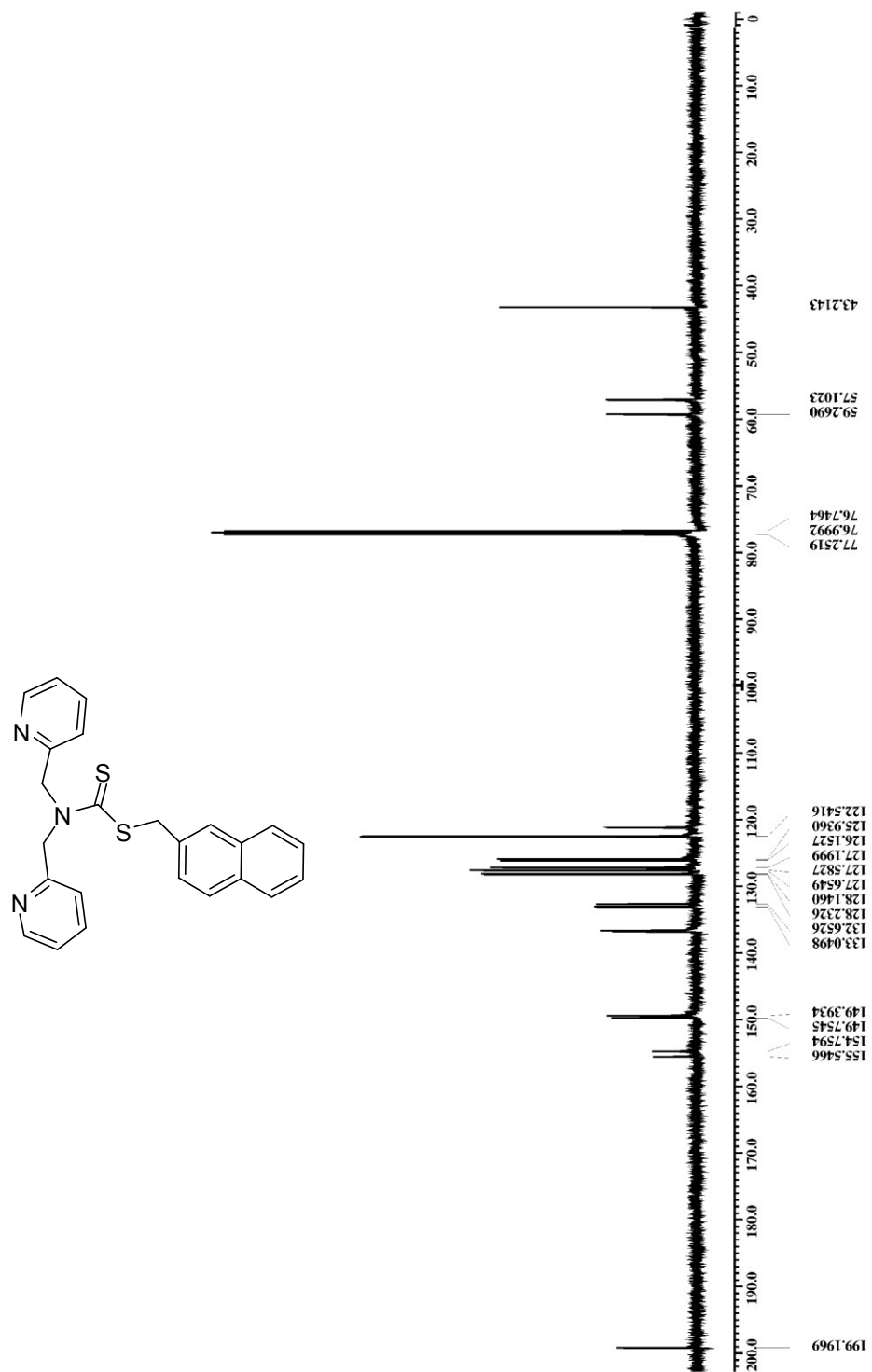


Figure S25. ^{13}C NMR spectrum of 1.

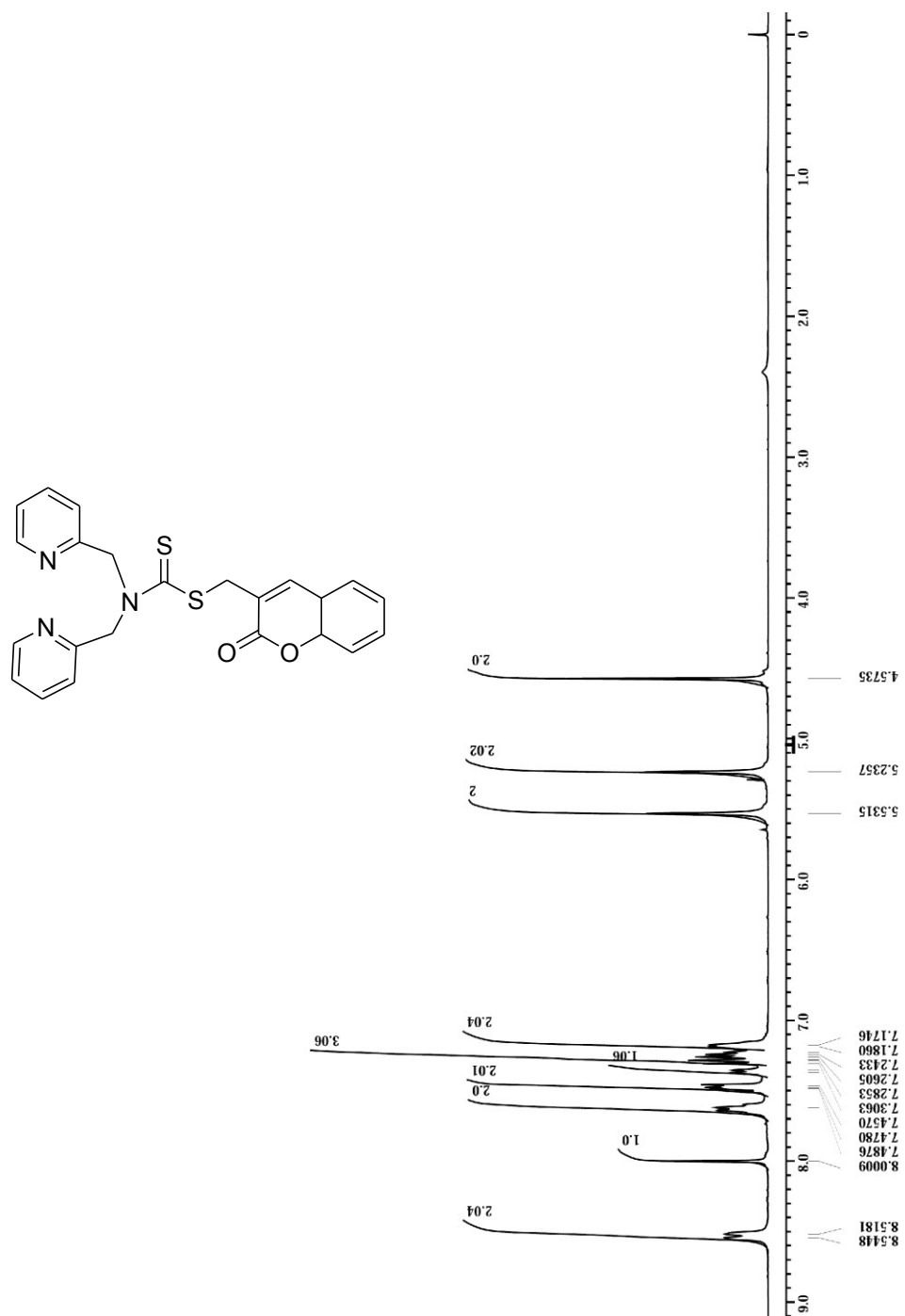


Figure S26. ¹H NMR spectrum of 2

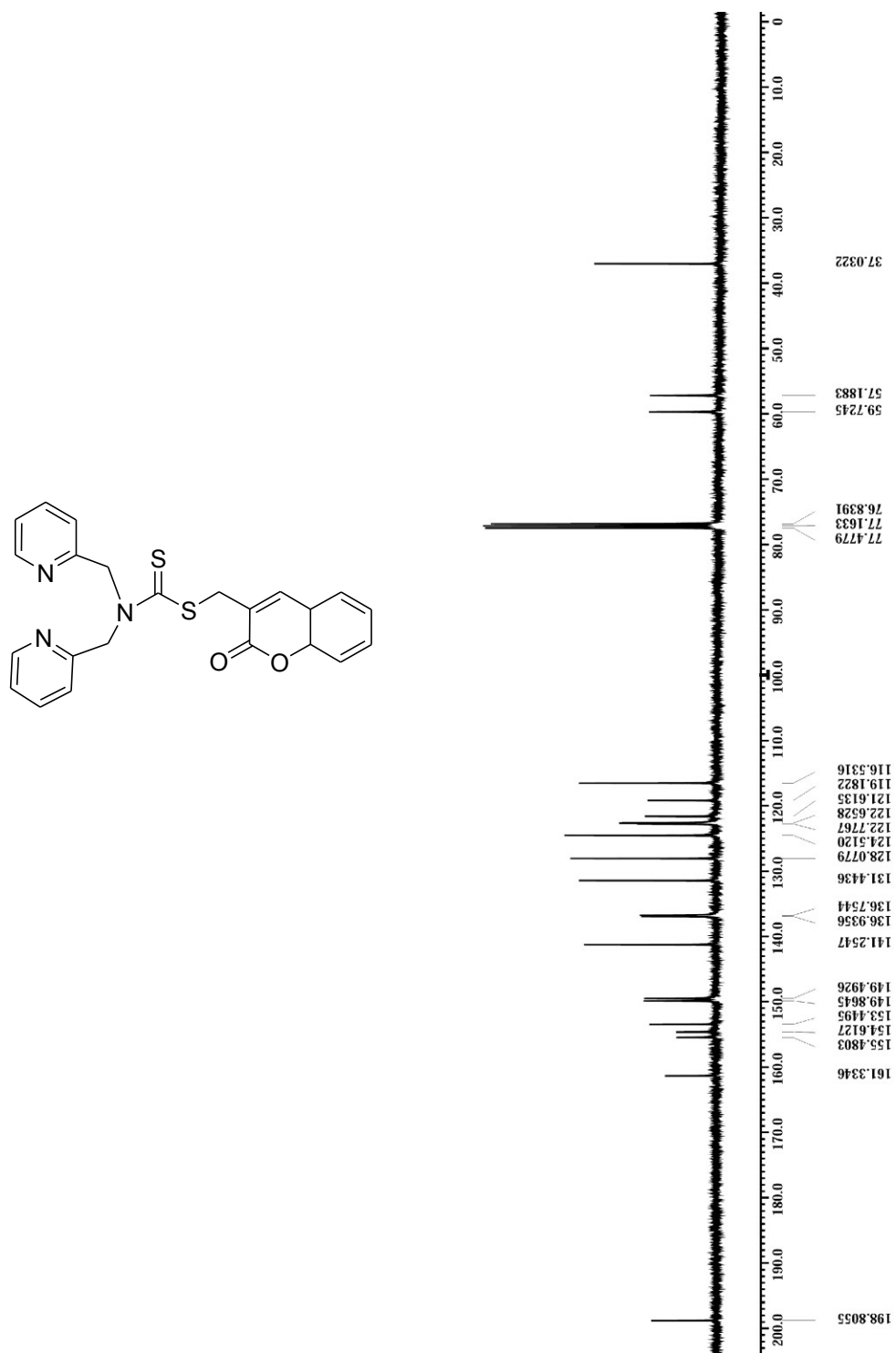


Figure S27. ^{13}C NMR spectrum of 2.

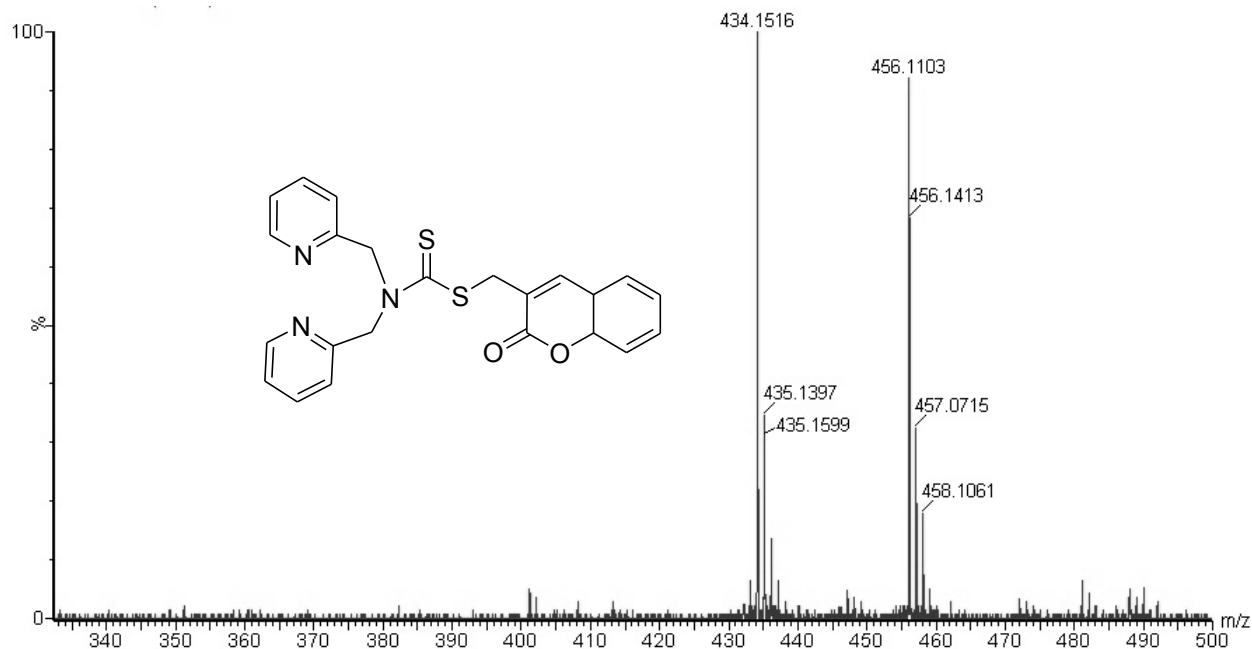


Figure S28. ESI-MS of **2** showing $[M + H]^+$ and $[M+Na]^+$ peaks.

(1) For example: (a) J. Hatai, S. Pal, G. P. Jose and S. Bandyopadhyay, *Inorg. Chem.*, 2012, **51**, 10129; (b) J. Hatai, S. Pal and S. Bandyopadhyay, *RSC Adv.*, 2012, **2**, 10941; (c) J. Hatai, S. Pal, G. P. Jose, T. Sengupta and S. Bandyopadhyay, *RSC Adv.*, 2012, **2**, 7033.

(2) (a) J. Rosenthal and S.J. Lippard, *J. Am. Chem. Soc.*, 2010, **132**, 5536; (b) S. Mizukami, S. Okada, S. Kimura and K. Kikuchi, *Inorg. Chem.*, 2009, **48**, 7630; (c) Z. Xu, K.-H. Baek, H. N. Kim, J. Cui, X. Qian, D. R. Spring, I. Shin and J. Yoon, *J. Am. Chem. Soc.*, 2010, **132**, 601.

(3) (a) A. Caballero, R. Martinez, V. Lloveras, I. Ratera, J. Vidal-Gancedo, K. Wurst, A. Tarranga, P. Molina and J. Veciana, *J. Am. Chem. Soc.*, 2005, **127**, 15666; (b) M. Shortreed, R. Kopelman, M. Kuhn and B. Hoyland, *Anal. Chem.*, 1996, **68**, 1414; (c) W. Lin, L. Yuan, Z. Cao, Y. Feng and L. Long, *Chem. Eur. J.*, 2009, **15**, 5096.